

## Nitrogen-Rich Salts Based on the Energetic 5,5'-(Hydrazine-1,2-diyl)bis-[1H-tetrazolide] Anion

by Moritz Eberspächer, Thomas M. Klapötke\*, and Carles Miró Sabaté

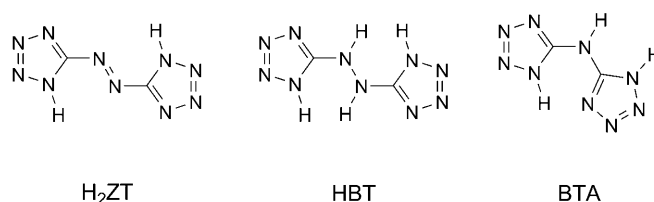
Department of Chemistry and Biochemistry, Ludwig-Maximilian University of Munich (LMU),  
Energetic Materials Research, Butenandstr. 5–13 (D), D-81377 Munich  
(e-mail: tmk@cup.uni-muenchen.de)

The reaction of 5,5'-(hydrazine-1,2-diyl)bis[1H-tetrazole] (HBT) with N-bases yielded a new family of energetic N-rich salts based on the 5,5'-(hydrazine-1,2-diyl)bis[1H-tetrazol-1-ide] anion with ammonium (see **1**), hydrazinium (see **2**), guanidinium (see **3**), and aminoguanidinium (see **4**) cations (5,5'-(hydrazine-1,2-diyl)bis[1H-tetrazol-1-ide] = 5,5'-(hydrazine-1,2-diyl)bis[tetrazolate]). All compounds were characterized by analytical and spectroscopic methods, and the crystal structure of **1** was determined by X-ray analysis (triclinic,  $P\bar{1}$ ). (Carboxyamino)guanidine betaine monohydrate (=2-(aminoiminomethyl)hydrazinecarboxylic acid hydrate (1:1); **5**) was obtained as a by-product in the synthesis of **4** and was characterized by X-ray analysis (monoclinic,  $P2_1/c$ ). Differential-scanning calorimetric (DSC) measurements were used to assess the thermal behavior of the energetic salts **1–4**, and bomb calorimetry allowed us to determine the experimental constant-volume energies of formation ( $\Delta_c U_{\text{exp}}$ ). In addition, the detonation parameters (pressure and velocity) were calculated from the energies of formation (back-calculated from  $\Delta_c U_{\text{exp}}$ ) with the EXPLO5 code, and their validity was checked by comparison with the results obtained from theoretical constant-volume energies of formation ( $\Delta_c U_{\text{pred}}$ ) obtained by means of quantum-chemical calculation (MP2) of electronic energies and an approximation of lattice enthalpy. Lastly, the sensitivity to shock, friction, and electrostatic discharge of **1–4** was measured by submitting the compounds to standard tests, and the ICT code was used to predict the products formed upon decomposition of the salts.

**1. Introduction.** – N-Rich chemistry is one of the milestones of energetic materials of the future [1–4]. Compounds with high N-contents have highly positive heats of formation and high densities both of which are associated to the energetic N–N and C–N bonds in the molecule [5]. In addition, such materials are interesting for applications requiring environmentally friendly energetic compounds since the main decomposition product will be molecular  $N_2$ . Other criteria to keep in mind when designing new compounds with prospective energetic applications relate to the performance, sensitivity, stability, and compatibility (*e.g.*, binder) of the material as well as to the associated cost for its synthesis [6]. Energetic compounds with high performance and decreased sensitivity to classical stimuli (*i.e.*, impact and friction) are sought. However, these two parameters are often playing against each other [7]. One way of counteracting the correlation of high detonation parameters (high performance) with high sensitivity is the use of systems which form extensive H-bonding networks in the solid state since the material is stabilized by substantial H-bonding [8][9]. In this context, salt-based energetic materials are generally preferred since they tend to exhibit lower vapor pressures, thus diminishing the risk of exposure through inhalation in comparison to neutral compounds with similar structures [7][10]. Ionic

energetic materials based on amines, hydrazines, and guanidines are known to form strong H-bonding networks and can show remarkable stability and considerable insensitivity to physical stimuli as well as good explosive performance [11].

In this context, azole- and in particular tetrazole-based energetic materials seem to show the best compromise between high performance, low sensitivity, and moderate thermal stability [12]. An energetically interesting compound is the free acid 5,5'-azobis[1*H*-tetrazole] ( $H_2ZT$ ; *Fig. 1*) [5]. However, its high lability is in contrast with the high stability of the parent 5,5'-(hydrazine-1,2-diyl)bis[1*H*-tetrazole] (= 5,5'-(hydrazine-1,2-diyl)bis[2*H*-tetrazole]; HBT) as established by recent work in our group [6][13]. HBT was first reported more than a century ago by *Thiele* [14] and was studied later on by *Spear* and *Elischer* as an energetic sensitizer [15]. However, the compound had hardly been characterized, and the energetic properties remained unreported. The energetic properties of metal salts of  $H_2ZT$  [16] and of the parent bis(1*H*-tetrazol-5-yl)amine (= *N*-(2*H*-tetrazol-5-yl)-2*H*-tetrazol-5-amine; BTA) [17] have been studied recently. Some salts of  $H_2ZT$  have found practical application in gas generators for airbags as well as in fire-extinguishing systems [2a][18][19], initiators [16], or in solid-rocket propellants [17]. Also recently, we reported the energetic properties of N-rich salts of  $H_2ZT$  [20], which were complemented by recent work of *Shreeve* and co-workers on similar salts of BTA [21]. Metal salts of  $H_2ZT$  and BTA have, in general, good thermal stabilities, whereas the corresponding N-rich salts are high-performing materials. Our most recent studies [6][13] showed that HBT is an N-rich energetic compound with excellent stability and sensitivity properties and an exceptional performance comparable to some of the highest performing commonly used explosives. Apart from preliminary results on the synthesis and characterization [22] and thermal studies of salts of HBT [22][23], very little is known about the potential of metal and N-rich salts containing the  $HBT^{2-}$  anion. With all this in mind, we decided to investigate N-rich (ammonium, hydrazinium, and guanidinium-based) salts of HBT as potential new energetic materials with high performance and low sensitivity [21][22].

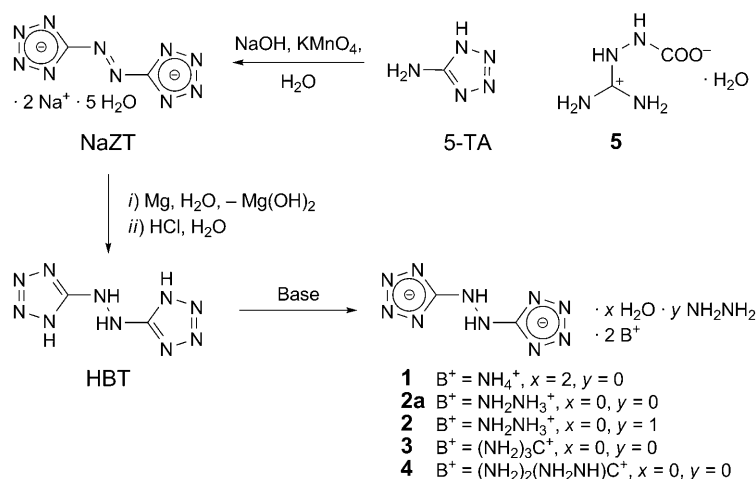


*Fig. 1.* N-Rich compounds 5,5'-azobis[1*H*-tetrazole] ( $H_2ZT$ ), 5,5'-(hydrazine-1,2-diyl)bis[1*H*-tetrazole] (HBT), and bis(1*H*-tetrazol-5-yl)amine (BTA)

**2. Synthesis.** – The 1*H*-tetrazol-5-amine (= 2*H*-tetrazol-5-amine; 5-TA) was oxidized in NaOH solution by  $KMnO_4$  yielding disodium 5,5'-azobis[1*H*-tetrazol-1-ide]<sup>1</sup>) pentahydrate ( $Na_2ZT$ ) [24], which was transformed further into the starting material 5,5'-(hydrazine-1,2-diyl)bis[1*H*-tetrazole] (HBT) [6][13]. The free acid HBT is a strong acid and can accordingly be deprotonated by a suitable base. Thus, we

<sup>1</sup>) Formerly, a bis[1*H*-tetrazol-1-ide] (=bis[2*H*-tetrazole] ion (2<sup>-</sup>)) was called bis[tetrazolate].

synthesized salts containing the  $\text{HBT}^{2-}$  anion and N-rich cations such as ammonium (see **1**), hydrazinium (see **2**), guanidinium (see **3**) and aminoguanidinium (see **4**) by acid–base reactions (Scheme 1). The ammonium salt was formed as the dihydrate species **1**. The hydrazinium salt **2a** was obtained as the solvate-free species (see *Exper. Part*), when the reaction was carried out in  $\text{H}_2\text{O}$ ; however, when 99% hydrazine hydrate was used as the solvent, this yielded the previously reported monohydrazine compound **2**, which has an even higher N-content of 84.7%. This is an interesting observation, which is in keeping with metal salts of the same anion [22]. In addition, the use of 99% hydrazine hydrate instead of the highly explosive anhydrous hydrazine, as reported previously, offers a clear advantage for the synthesis of **2** [22]. The synthesis of **4** produced crystals of a by-product, which was identified by its *Raman* spectrum and X-ray crystal-structure analysis as (carboxyamino)guanidine betaine monohydrate (**5**; see molecular-structure discussion, *Sect. 3.3*). This betaine turned out to be one of the starting materials of the synthesis of **4**, which was purchased under the name of aminoguanidinium hydrogen carbonate [25]. Since a suitable source of the N-richer diamino- and triaminoguanidinium cations is not readily available, the synthesis of the corresponding compounds was not feasible. On the one hand, reaction of disilver 5,5'-(hydrazine-1,2-diyl)bis[1*H*-tetrazol-1-ide] with the corresponding halogenide salt did not result in the expected precipitation of a silver halide due to the high insolubility of the silver salt, which is in contrast to the synthesis of analogous salts of BTA from disilver 5,5'-iminobis[1*H*-tetrazol-1-ide] ( $\text{BTA}^{2-} \cdot 2 \text{Ag}^+$ ) [26]. On the other hand, reaction between a guanidinium sulfate salt and barium 5,5'-(hydrazine-1,2-diyl)-bis[1*H*-tetrazol-1-ide] [27] only resulted in the isolation of the impure desired compound, in contrast to salts of BTA prepared by an analogous method [21].

Scheme 1. Synthesis of 5,5'-(Hydrazine-1,2-diyl)bis[1*H*-tetrazole] Derivatives

The synthesis of the salts containing the  $\text{HBT}^{2-}$  anion needs to be carried out under  $\text{N}_2$  due to the facile oxidation of the compounds to the 5,5'-azobis[tetrazolide] salts ( $\text{ZT}^{2-}$ ) in solution, whereas in the solid state the compounds are much more stable (see energetic-properties, discussion, *Sect. 3.4*).

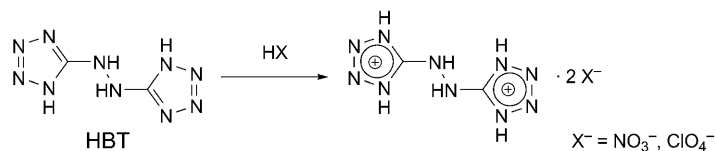
**3. Characterization.** – 3.1. *Analytical and NMR-Spectroscopic Properties of 1–4.* All compounds were characterized by elemental analysis (see *Exper. Part*) and mass spectrometry and by spectroscopic methods (IR/Raman and  $^1\text{H}$ - and  $^{13}\text{C}$ -NMR). *Table 1* shows a summary of the corresponding data of the salts **1–4**.

Table 1. *Characterization of the N-Rich 5,5'-(Hydrazine-1,2-diyl)bis[1H-tetrazol-1-ide] Salts 1–4*

	<b>1</b>	<b>2</b>	<b>3</b>	<b>4</b>
$^1\text{H}$ -NMR [ppm]	7.8 (NHNH), 5.5 ( $\text{NH}_4^+$ )	8.0 (NHNH), 5.9 ( $\text{H}_2\text{NNH}_3^+$ )	7.1 ( $\text{C}=\text{NH}_2^+$ , HNNH)	7.7 ( $\text{C}=\text{NH}_2^+$ , NHNH), 7.1 (NH), 4.8 ( $\text{NH}_2$ )
$^{13}\text{C}$ -NMR [ppm]	164.7 ( $\text{C}_{\text{ring}}$ )	167.4 ( $\text{C}_{\text{ring}}$ )	157.8 ( $\text{C}=\text{NH}_2^+$ ), 167.9 ( $\text{C}_{\text{ring}}$ )	158.6 ( $\text{C}=\text{NH}_2^+$ ), 167.9 ( $\text{C}_{\text{ring}}$ )
IR [ $\text{cm}^{-1}$ ]	1426, 1376	1466, 1365	1360	1457
Raman [ $\text{cm}^{-1}$ ]	1074	1056	1060	1048
MS (FAB, pos.)	18 ( $\text{NH}_4^+$ )	33.1 ( $\text{N}_2\text{H}_5^+$ )	60 ( $\text{CH}_6\text{N}_3^+$ )	75 ( $\text{CH}_7\text{N}_4^+$ )
MS (FAB, neg.)	167 ( $\text{C}_2\text{H}_3\text{N}_{10}^+$ )	167 ( $\text{C}_2\text{H}_3\text{N}_{10}^+$ )	167 ( $\text{C}_2\text{H}_3\text{N}_{10}^+$ )	167 ( $\text{C}_2\text{H}_3\text{N}_{10}^+$ )
DSC [ $^\circ$ ; $5^\circ \text{ min}^{-1}$ ]	111 ( $-\text{H}_2\text{O}$ ), 196 (dec.)	154–182 (m.p., dec.)	214 (dec.)	142–194 (m.p., dec.)

HBT exhibits only one averaged signal at  $\delta$  9.6 in the  $^1\text{H}$ -NMR spectrum ( $(\text{D}_6)$ DMSO) arising from the fast exchange in this solvent [13]. This resonance is shifted to low field in comparison to 1*H*-tetrazol-5-amine (5-TA), which is indicative of the acid character of the ring H-atom in HBT and explains the failure of the synthesis of the corresponding nitrate and perchlorate salts of HBT (*Scheme 2*). Direct reaction between HBT and nitric acid resulted in the formation of a yellow solution pointing at oxidation of the hydrazinediyl moiety to the azo linker. Unexpectedly, although perchloric acid is a stronger acid and more oxidizing than nitric acid, reaction with HBT did not result in oxidation of the hydrazinediyl linker, and HBT was recovered from the reaction mixture. However, HBT was easily deprotonated with N-bases to form compounds **1–4** (see above), which experience a high-field shift of the H-atoms of the hydrazinediyl moiety to  $\delta$  ca. 7.0–8.0.

Scheme 2. *Attempted Synthesis of Salts of the HBT<sup>2+</sup> Cation*



The free acid HBT shows a  $^{13}\text{C}$ -NMR resonance for the ring C-atoms at  $\delta$  159.6, which is shifted to high field by comparison to salts of the 5,5'-azobis[1*H*-tetrazol-1-ide] anion ( $\delta$  ca. 173) [16] and which is in keeping with salts of 1*H*-tetrazol-5-amine [12b][28]. In the  $^{13}\text{C}$ -NMR spectra of the salts **1–4**, this resonance is observed at lower field ( $\delta$  ca. 165–168) than that of HBT as a consequence of the deshielding effect produced by the delocalization of the negative charge but still at higher field than that of analogous 5,5'-azobis[1*H*-tetrazol-1-ide] salts [16]. As mentioned above, salts of HBT are readily oxidized in solution to the azo compounds, and this can be monitored

by  $^{13}\text{C}$ -NMR where the ring –C-atom resonance at  $\delta$  ca. 167 slowly disappears and is replaced by a signal at  $\delta$  ca. 173. In addition, a color change of the solution from colorless to yellow is also indicative of oxidation to form the  $\text{ZT}^{2-}$  salt.

Lastly, in the  $^{14}\text{N}$ -NMR spectra of **1–4** only broad signals arising from the quadrupole moment of this nucleus are observed. Unfortunately, the solubility of all salts in common solvents was too low to allow to record a  $^{15}\text{N}$ -NMR spectrum (natural abundance). Similarly to the spectra recorded in solution, in the solid-state  $^{15}\text{N}$ -NMR experiments, the spectra of **1–4** are characterized by broad bands, and the only resonance which can be assigned is that of the hydrazinediyl N-atoms ( $\delta$  ca. – 297). The free acid HBT, in contrast, shows well-defined resonances in the solid-state  $^{15}\text{N}$ -NMR spectrum [13].

3.2. *Vibrational Spectroscopy.* Deprotonation of HBT to yield the  $\text{HBT}^{2-}$  anion of the salts **1–4** results in obvious differences in the IR and Raman shifts. Except for some shift variations, all spectra look very similar, as expected from the similarities of the anion structure. The N–H region for all four salts is characterized by bands of medium intensity with maxima at ca. 3140 and ca. 3000  $\text{cm}^{-1}$  in the IR spectra, corresponding to N–H stretching modes in the anion and in the cation, respectively. However, the most intense signals in the IR spectra of all salts are found at ca. 1370 and ca. 1450  $\text{cm}^{-1}$  due to coupled deformation modes of the hydrazinediyl-linker and ring stretches. In addition, the in-the-plane C–N (hydrazinediyl) stretch (C(1)–N(5); for atom numbering, see below, Fig. 3) is observed within a relatively wide range (1615–1645  $\text{cm}^{-1}$ ) and is Raman inactive. In the Raman spectra, instead, the most intense signals are observed in the range 1048–1074  $\text{cm}^{-1}$  for the different compounds and correspond to stretching vibrations in the two tetrazole rings. Lastly, many other signals of lower intensity can be assigned as follows: 720–770  $\text{cm}^{-1}$  ( $\omega(\text{HN–NH})$ ), 800–860  $\text{cm}^{-1}$  ( $\delta(\text{HN–NH})$ ), 1100–1125  $\text{cm}^{-1}$  ( $\tilde{\nu}(\text{N–N})_{\text{ring}}$ ), ca. 1370  $\text{cm}^{-1}$  ( $\delta(\text{HN–NH})_{\text{ip}}$  and  $\tilde{\nu}(\text{N–N})_{\text{ring}}$ ), 1360–1380  $\text{cm}^{-1}$  ( $\delta(\text{HN–NH})_{\text{oop}}$  and  $\tilde{\nu}(\text{N–N})_{\text{ring}}$ ), 1440–1460  $\text{cm}^{-1}$  ( $\delta(\text{HN–NH})_{\text{ip}}$  and  $\tilde{\nu}(\text{N–N})_{\text{ring}}$ ) and 1510–1550  $\text{cm}^{-1}$  ( $\delta(\text{HN–NH})_{\text{ip}}$  and  $\tilde{\nu}(\text{C–N})_{\text{ring}}$ ) [2b][29].

3.3. *Molecular Structures of 1 and 5.* In Table 2, the X-ray crystal-structure solution and refinement data for both compounds **1** and **5** are summarized. Selected bond lengths and angles are reported in Tables 3 and 5 for **1** and **5**, respectively. In addition, the distances and angles of the H-bonds are given in Table 4.

According to the single-crystal X-ray diffraction, the N–N bond distances in the anion of **1** (1.308(3)–1.441(4) Å) are between N–N single bonds (1.454 Å) and N=N bonds (1.245 Å) (Table 3)<sup>2)</sup>. This indicates conjugation of the negative charge throughout the aromatic rings as seen in the crystal structures of other salts containing the same anion [22][27]. The distance between the two linker N-atoms of **1** (N(5)–N(5)<sup>(iv)</sup> = 1.441(4) Å) is relatively long (N–N = 1.454 Å<sup>2)</sup>) [31], longer by ca. 0.06 Å than the analogous N–N distance observed in the free acid HBT [6][13], in which no conjugation between the two aromatic rings and the linking N-atoms is observed.

The salt **1** crystallizes as the dihydrated species forming nonplanar layers as represented in Fig. 2, which are connected by H-bonds to H<sub>2</sub>O molecules and NH<sub>4</sub><sup>+</sup>

<sup>2)</sup> N–N and N=N bond distances from [30].

Table 2. X-Ray Crystal-Structure Solution and Refinement for Compounds **1** and **5**

	<b>1</b>	<b>5</b>		<b>1</b>	<b>5</b>
Molecular Formula	C <sub>2</sub> H <sub>14</sub> N <sub>12</sub> O <sub>2</sub>	C <sub>2</sub> H <sub>8</sub> N <sub>4</sub> O <sub>3</sub>	$\rho_{\text{calc.}}$ [g/cm <sup>3</sup> ]	1.544	1.550
$M_r$	238.26	136.12	$\mu$ [mm <sup>-1</sup> ]	0.130	0.144
Crystal size [mm]	0.25 × 0.10 × 0.10	0.20 × 0.10 × 0.10	$F(000)$	126	288
Crystal system	triclinic	monoclinic	$\theta$ range [°]	3.94–27.00	3.72–25.98
Space group	$P-1$	$P2_1/c$	$\lambda$ (MoK $\alpha$ ) [Å]	0.71073	0.71073
$a$ [Å]	3.8236(2)	9.1213(6)	Temp. [K]	200(2)	200(2)
$b$ [Å]	6.9671(5)	4.8400(3)	Index range	$-4 \leq h \leq 4$ , $-8 \leq k \leq 8$ , $-12 \leq l \leq 12$	$-11 \leq h \leq 11$ , $-5 \leq k \leq 5$ , $-16 \leq l \leq 16$
$c$ [Å]	9.9199(6)	13.2259(8)	Refl. collected	5803	5542
$\alpha$ [°]	80.478(5)	90	Refl. unique	1107	1140
$\beta$ [°]	88.652(4)	92.779(6)	$R$ (int.)	0.0236	0.0357
$\gamma$ [°]	79.478(5)	90	Data, restr., param.	1107, 0, 109	1140, 0, 114
$V$ [Å <sup>3</sup> ]	256.23(3)	583.20(6)	g.o.f.	1.287	0.997
$Z$	1	4	$R_1^a$ , $wR_2$ ( $I > 4\sigma(I)$ )	0.0488, 0.1191	0.0283, 0.0672
			$R_1$ , $wR_2$ (all data)	0.0566, 0.1207	0.0483, 0.0770

<sup>a</sup>)  $R_1 = \sum ||F_o| - |F_c|| / \sum |F_o|$ .  $R_w = [\sum (F_o^2 - F_c^2) / \sum w (F_o^2)]^{1/2}$ .  $w = [\sigma_c^2 Z (F_o^2) + (xP)^2 + yP]^{-1}$ ,  $P = (F_o^2 - 2F_c^2) / 3$ .

Table 3. Bond Distances and Angles in 5,5'-(Hydrazine-1,2-diyl)bis[1H-tetrazol-1-ide] Salt **1**. See Fig. 3 for atom numbering.

Bond [Å]	Bond [Å]	Angle [°]	Angle [°]
C(1)–N(1) 1.329(3)	N(4)–C(1) 1.331(3)	N(3)–N(2)–N(1) 109.5(2)	N(1)–C(1)–N(5) 125.9(2)
N(1)–N(2) 1.356(3)	C(1)–N(5) 1.409(3)	N(2)–N(3)–N(4) 109.7(2)	C(1)–N(1)–N(2) 103.9(2)
N(2)–N(3) 1.308(3)	N(5)–N(5) <sup>(iv)a</sup> 1.441(4)	N(4)–C(1)–N(1) 112.9(2)	C(1)–N(4)–N(3) 104.0(2)
N(3)–N(4) 1.350(3)		N(4)–C(1)–N(5) 121.2(2)	C(1)–N(5)–N(5) <sup>(iv)a</sup> 110.9(2)

<sup>a</sup>) Symmetry code: (iv)  $2 - x, 1 - y, -z$ .

cations. Similarly to other compounds containing the HBT<sup>2-</sup> anion, there exists disorder in the structure. The average configuration of the anion presents tetrazole rings which its on parallel planes. When one of the protons at N(5) points upwards, the H-atom at N(5)<sup>(iv)</sup> (symmetry code: (iv)  $2 - x, 1 - x, -z$ ) points downwards and *vice versa* (i.e., the H-atoms on the hydrazinediyl linker are only half occupied). In the difference Fourier electron-density map, three small electron densities can be found in the vicinity of the O-atoms of the H<sub>2</sub>O molecules, which can be assigned to three protons: two of which have approximately half occupied positions (49 and 51%) and one with a fully occupied position.

Fig. 3 shows the H-bonding in the structure of **1**. Every N-atom is involved in the formation of H-bonds of different strength (see Table 4). In one of the two possible configurations adopted by **1**, H<sub>2</sub>O molecules are H-bond donors interacting with the hydrazinediyl-linker N-atoms with  $O \cdots N(5) = 2.942(3)$  Å, and in the other config-

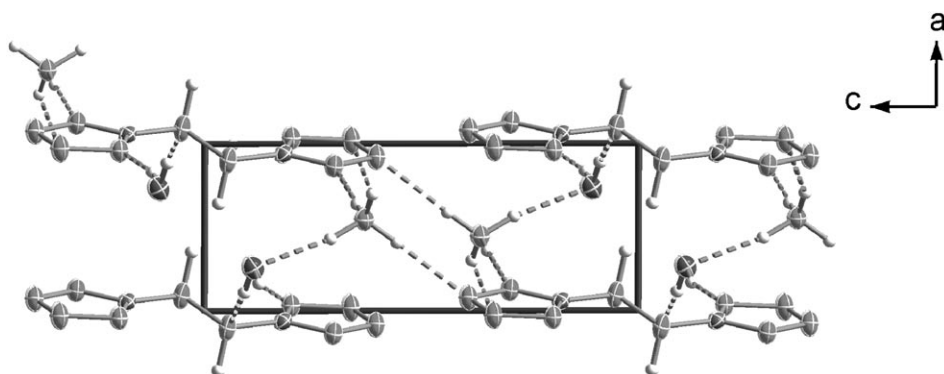
Table 4. *Hydrogen-Bonding Geometry in 5,5'-(Hydrazine-1,2-diyl)bis[1H-tetrazol-1-ide] Salt 1*. See Fig. 3 for atom numbering.

D–H...A	D–H [Å]	H...A [Å]	D...A [Å]	D–H...A [°]
<b>1</b> : O–H(2)...N(5)	0.88(4)	2.09(3)	2.942(3)	162(3)
N(5)–H(5A)...O	0.91(4)	2.00(4)	2.932(3)	168(3)
N(6)–H(6A)...N(4)	0.91(4)	1.94(3)	2.884(3)	171(3)
N(6)–H(6B)...O <sup>(i)a</sup>	0.90(3)	1.91(3)	2.833(3)	170(3)
N(6)–H(6D)...N(3) <sup>(ii)a</sup>	0.90(4)	2.04(4)	2.942(3)	174(3)
N(6)–H(6C)...N(2) <sup>(iii)a</sup>	0.87(3)	2.16(4)	2.966(3)	154(3)
O–H(1)...N(1) <sup>(iii)a</sup>	0.84(4)	2.06(3)	2.791(3)	162(3)
<b>5</b> : N(1)–H(4)...N(4)	0.84(2)	2.41(2)	2.710(2)	102(1)
N(3)–H(5)...O(3)	0.88(2)	1.91(2)	2.826(2)	169(1)
N(4)–H(6)...O(1) <sup>(iv)b</sup>	0.85(2)	2.07(2)	2.910(2)	170(1)
O(3)–H(7)...O(2) <sup>(ii)b</sup>	0.94(2)	1.78(2)	2.723(2)	175(2)
N(2)–H(2)...O(3) <sup>(iii)b</sup>	0.87(2)	2.13(2)	2.944(2)	156(2)
N(2)–H(1)...O(2) <sup>(iv)b</sup>	0.88(2)	2.01(2)	2.885(2)	176(2)
N(1)–H(3)...O(1) <sup>(iv)b</sup>	0.94(2)	1.92(2)	2.854(2)	174(1)
O(3)–H(8)...O(2) <sup>(v)b</sup>	0.83(2)	1.94(2)	2.768(2)	178(2)
N(1)–H(4)...O(1) <sup>(vi)b</sup>	0.84(2)	2.15(2)	2.904(2)	150(2)

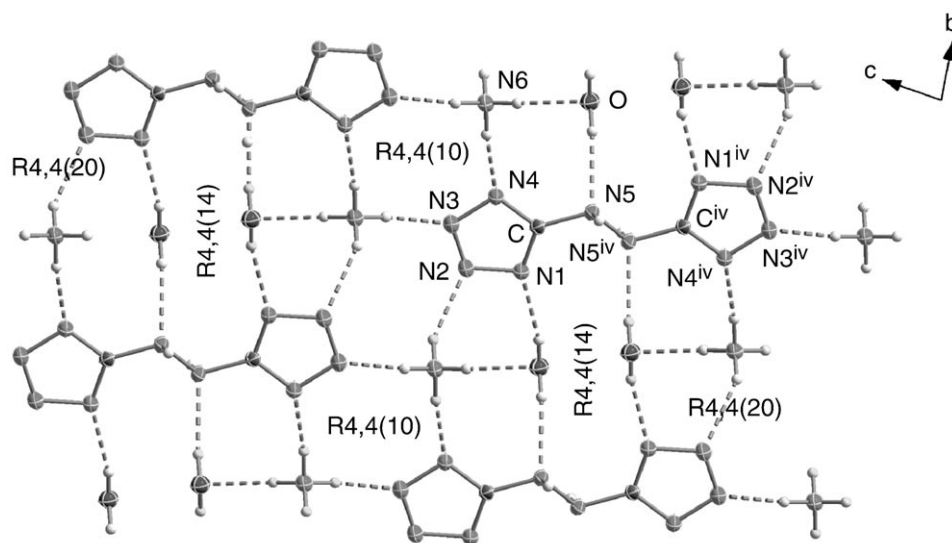
<sup>a</sup>) Symmetry codes for **1**: (i)  $x+1, y, z$ ; (ii)  $-x+3, -y+1, -z+1$ ; (iii)  $x, y+1, z$ . <sup>b</sup>) Symmetry codes for **5**: (i)  $2-x, 0.5+y, 0.5-z$ ; (ii)  $x, 1+y, z$ ; (iii)  $1-x, 1-y, -z$ ; (iv)  $x, -0.5-y, -0.5+z$ ; (v)  $1-x, 0.5+y, 0.5-z$ ; (vi)  $2-x, -0.5+y, 0.5-z$ .

Table 5. *Bond Distances and Angles in Betaine 5*. See Fig. 4 for atom numbering.

Bond [Å]	Bond [Å]	Bond [Å]	Angle [°]	Angle [°]
N(4)–C(2) 1.376(2)	C(1)–N(1) 1.317(2)	C(2)–N(4)–N(3) 121.4(1)	N(2)–C(1)–N(3) 118.4(1)	
N(4)–N(3) 1.386(2)	C(2)–O(1) 1.258(2)	C(1)–N(3)–N(4) 119.8(1)	O(1)–C(2)–O(2) 125.6(1)	
N(3)–C(1) 1.344(2)	C(2)–O(2) 1.267(2)	N(1)–C(1)–N(2) 120.8(1)	O(1)–C(2)–N(4) 115.8(1)	
N(2)–C(1) 1.321(2)		N(1)–C(1)–N(3) 120.6(1)	O(2)–C(2)–N(4) 118.4(1)	

Fig. 2. *View of the unit cell of 1 along the b-axis showing the formation of nonplanar layers connected by H-bonding (dotted lines)*

uration, they accept a H-bond from the hydrazinediyl-linker N-atoms with  $N(5) \cdots O = 2.932(3) \text{ \AA}$ . By means of the graph-set formalism introduced by *Bernstein, Davies*, and co-workers [31] and the computer program RPLUTO [32], one of the two possible configurations (represented in *Fig. 3*) can be described as forming dimeric interactions of the type **D1,1(2)** and **C1,1(3)** chain motifs, which combine at the primary level with themselves to form finite patterns with the label **D2,2(X)** ( $X = 4, 8, 10$ ) and **C2,2(6)** chain graph sets, respectively. At the secondary level, many **D2,2(X)** ( $X = 4-9$ ) finite patterns, **C2,2(X)** ( $X = 6, 10, 11$ ) and **C2,3(5)** and **C3,3(X)** ( $X = 7, 9, 11, 13$ ) chain networks, and **R4,4(X)** ( $X = 10, 14, 20$ ) ring graph sets are found. For example, the **R4,4(10)** motifs are formed by the interaction of two  $\text{HBT}^{2-}$  anions *via* two  $\text{NH}_4^+$  cations ( $N(6) \cdots N(3)^{(ii)} = 2.942(3)$  and  $N(6) \cdots N(2)^{(iii)} = 2.966(3) \text{ \AA}$ ; symmetry codes: (ii)  $-x + 3, -y + 1, -z + 1$ ; (iii)  $x, y + 1, z$ ). The **R4,4(14)** graph sets are generated by the interaction of two anions with two  $\text{H}_2\text{O}$  molecules *via* the H-bond between O and N(5) mentioned above and the shortest contact in the structure ( $O \cdots N(1)^{(iii)} = 2.791(3) \text{ \AA}$ ). Lastly, the **R4,4(20)** patterns are formed by the interaction of two  $\text{NH}_4^+$  cations with N(2) and N(4) of the anion.



*Fig. 3.* H-Bonding in the crystal structure of **1** with the labeling scheme (arbitrary) showing the formation of some characteristic graph sets (symmetry code: (iv)  $2 - x, 1 - y, -z$ )

The crystal structure of betaine **5** has already been reported by *Kolev and Petrova* [25]; therefore, only details not discussed before will be pointed out here. As shown in *Fig. 4*, **5** undergoes extensive H-bonding. The noncoplanarity between the  $\text{CN}_3$  and the  $\text{CO}_2\text{N}$  moieties does not allow the formation of planar layers, and the molecules are linked by a relatively strong three-dimensional H-bonded network. Once more, the graph-set nomenclature facilitates the identification of such a complex network. Every molecule of **5** is involved in the formation of up to nine H-bonds (*Table 4*), one of which is intramolecular ( $N(1) \cdots N(4) = 2.710(2) \text{ \AA}$ ) and forms an **S(5)** intramolecular pattern (not represented in *Fig. 4* for the sake of simplicity) and the rest form several



**D1,1(2)** finite patterns and **C1,1(X)** ( $X=4,7$ ) chain graph sets, all of them at the primary level. At the secondary level, there exist finite chain patterns of the type **D2,3(10)** and **D3,3(X)** ( $X=9, 11, 12, 14, 15$ ), chain networks with the labels **C1,2(X)** ( $X=4, 7$ ) and **C2,2(X)** ( $X=7, 9, 14$ ), and most interestingly ring graph sets of the form **R2,2(X)** ( $X=7, 8, 11$ ), **R2,4(X)** ( $X=8, 12, 14$ ), and **R4,4(X)** ( $X=16, 18, 22, 28$ ). Some of these ring H-bonding networks are represented in Fig. 4. For example, four molecules of **5** H-bond each other to form an **R2,4(8)** ring pattern ( $N(1) \cdots O(1)^{(iv)} = 2.854(2) \text{ \AA}$  and  $N(1) \cdots O(1)^{(vi)} = 2.904(2) \text{ \AA}$ ; symmetry codes: (iv)  $x, -0.5 - y, -0.5 + z$ ; (vi)  $2 - x, -0.5 + y, 0.5 - z$ ), or two molecules of **5** are linked *via*  $H_2O$  molecules to form **R2,4(12)** patterns ( $N(3) \cdots O(3) = 2.826(2) \text{ \AA}$  and  $N(2) \cdots O(3)^{(iii)} = 2.944(2) \text{ \AA}$ ; symmetry code: (iii)  $1 - x, 1 - y, -z$ ).

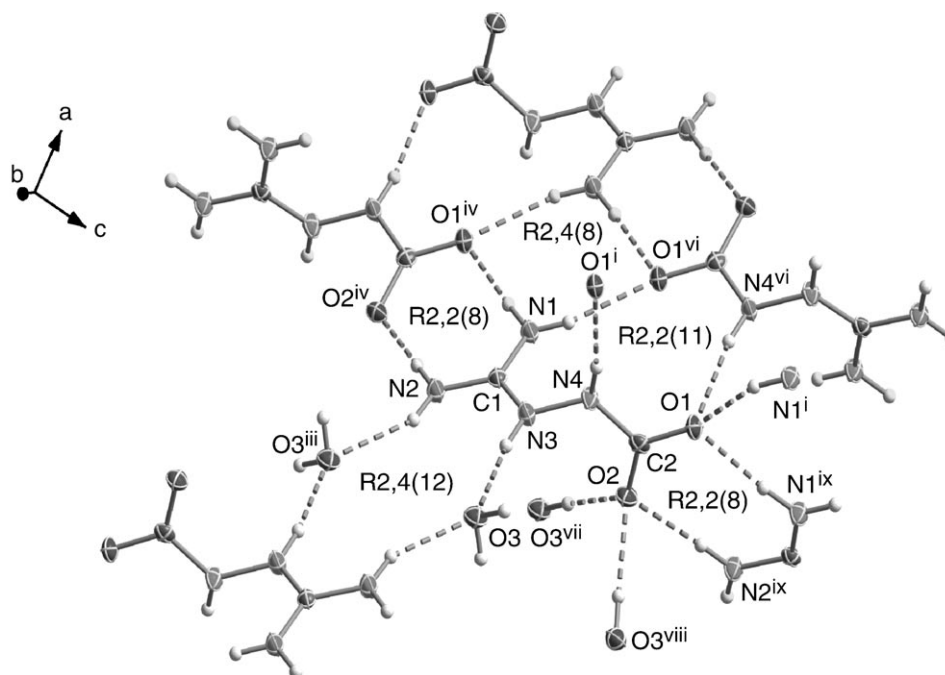
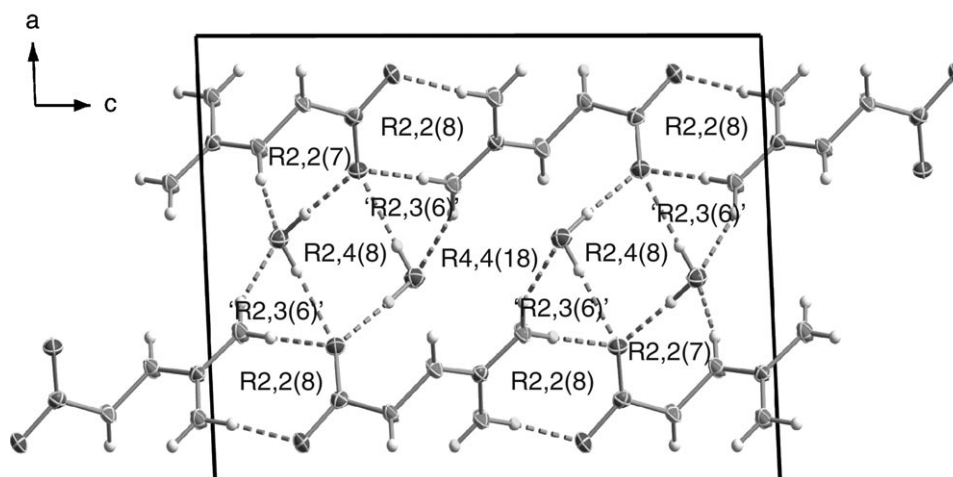


Fig. 4. Labeling scheme (arbitrary) and H-bonding in the crystal structure of **5** showing the formation of some characteristic graph sets (symmetry codes: (i)  $2 - x, 0.5 + y, 0.5 - z$ ; (iii)  $1 - x, 1 - y, -z$ ; (iv)  $x, -0.5 - y, -0.5 + z$ ; (vi)  $2 - x, -0.5 + y, 0.5 - z$ ; (vii)  $x, -1 + y, z$ ; (viii)  $1 - x, -0.5 + y, 0.5 - z$ ; (ix)  $x, -0.5 - y, 0.5 + z$ ). Parts of the structure and the intramolecular H-bond are not shown for the sake of simplicity.

Fig. 5 represents the H-bonding in the unit cell of **5**. Note that betaine molecules are linked over **R2,2(8)** graph sets ( $N(1) \cdots O(1)^{(iv)} = 2.854(2) \text{ \AA}$  and  $N(2) \cdots O(2)^{(iv)} = 2.885(2) \text{ \AA}$ ; symmetry code: (iv)  $x, -0.5 - y, -0.5 + z$ ) forming infinite chains along the crystallographic  $c$ -axis. Apart from the **R2,4(8)** networks discussed above between four molecules of **5**, there exist a second type of **R2,4(8)** patterns between betaine

molecules and bridging H<sub>2</sub>O molecules ( $O(3) \cdots O(2)^{(ii)} = 2.723(2) \text{ \AA}$  and  $O(3) \cdots O(2)^{(v)} = 2.768(2) \text{ \AA}$ ; symmetry codes: (ii)  $x, 1 + y, z$ ; (v)  $1 - x, 0.5 + y, 0.5 - z$ ). In addition, although RPLUTO is only restricted to find second-level graph sets, there exist at the tertiary level other ring networks with the designator **R2,3(6)** between one molecule of H<sub>2</sub>O and two of the betaine. Lastly, H<sub>2</sub>O molecules also link molecules of **5** to form the larger **R4,4(18)** ring pattern represented in *Fig. 5* by the H-bond  $N(2) \cdots O(3)^{(iii)} = 2.944(2) \text{ \AA}$  and that mentioned above between  $O(3)$  and  $O(2)^{(ii)}$ .



*Fig. 5.* View of the unit cell of **5** along the *b*-axis showing the formation of some characteristic graph sets

**3.4. Thermal Stability and Energetic Properties of N-Rich 5,5'-(Hydrazine-1,2-diyl)bis[1*H*-tetrazole] Derivatives.** The sensitivity to thermal stimuli of the N-rich compounds **1–4** was measured by differential-scanning calorimetry (DSC) at a heating rate of  $5^\circ \text{ min}^{-1}$ . The N-rich salts **1** and **3** of HBT with ammonium and guanidinium cations, respectively, decompose both at temperatures above  $190^\circ$ , and the crystal water in **1** is lost at *ca.*  $110^\circ$ , whereas the hydrazinium and aminoguanidinium salts **2** and **4**, respectively, show slow decomposition over a relatively broad range starting at *ca.*  $150^\circ$  (*Table 6*). *Fig. 1* of the supplementary material<sup>3)</sup> displays the results of the ‘flame test’ of salts **1** and **2** during two heating modalities. In the ‘fast-heating’ test, a few milligrams of the salt were loaded on a metal spatula, and this was put into direct contact with an open flame, whereas in the ‘slow-heating’ test, the spatula was held a few centimeters above the flame until a reaction was observed. The ‘fast-heating’ test revealed a fast reaction in all four cases **1–4**, whereas ‘slow heating’ of the salts resulted in a large deflagration without smoke, as expected from the high N-content of the materials.

*Table 7* summarizes the experimental results of the impact-, friction- and electrostatic-discharge sensitivity of the N-rich 5,5'-(hydrazine-1,2-diyl)bis[1*H*-tetrazol-1-ide] salts **1–4**. No detonation was observed in the drop-hammer test at  $> 30 \text{ J}$  nor at the

<sup>3)</sup> Supplementary material is available upon request from the author *T. M. K.*

Table 6. Physical and Chemical Properties of N-Rich 5,5'-(Hydrazine-1,2-diyl)bis[1*H*-tetrazole] Derivatives

	<b>1</b>	<b>2</b>	<b>3</b>	<b>4</b>
Formula	C <sub>2</sub> H <sub>14</sub> N <sub>12</sub> O <sub>2</sub>	C <sub>2</sub> H <sub>12</sub> N <sub>14</sub>	C <sub>4</sub> H <sub>14</sub> N <sub>16</sub>	C <sub>4</sub> H <sub>16</sub> N <sub>18</sub>
<i>M<sub>r</sub></i>	238.21	232.21	286.16	316.18
<i>T<sub>m</sub></i> [°] <sup>a</sup> )	–	154	–	142
<i>T<sub>d</sub></i> [°] <sup>b</sup> )	196	154–182	214	142–194
N [%] <sup>c</sup> )	70.6	84.5	78.3	79.7
<i>Ω</i> [%] <sup>d</sup> )	–60.4	–68.9	–96.8	–102.8
<i>ρ</i> [g cm <sup>–3</sup> ] <sup>e</sup> )	1.622	1.598 (picn.)	1.602 (picn.)	1.618 (picn.)
<i>Δ<sub>c</sub>U<sup>o</sup></i> [cal g <sup>–1</sup> ] <sup>f</sup> )	–3250(20)	–3320(15) (–3932)	–3280(15) (–3843)	–3390(20) (–3879)
<i>Δ<sub>f</sub>U<sup>o</sup></i> [kJ kg <sup>–1</sup> ] <sup>g</sup> )	2040(80) (4190)	3260(60) (5816)	1350(70) (3716)	2110(90) (4152)
<i>Δ<sub>f</sub>H<sup>o</sup></i> [kJ kg <sup>–1</sup> ] <sup>h</sup> )	1840(80) (3992)	3040(60) (5603)	1230(70) (3517)	1970(90) (3948)

<sup>a</sup>) Melting point and <sup>b</sup>) decomposition point (DSC onsets,  $\beta = 5^\circ \text{ min}^{-1}$ ). <sup>c</sup>) N-Atom percentage. <sup>d</sup>)  $\Omega = \text{O-balance}$  ([39]). <sup>e</sup>)  $\rho$  = density value from X-ray or picnometer (picn.) measurements. <sup>f</sup>)  $\Delta_c U^o$  = experimentally determined (oxygen-bomb calorimetry) energy of combustion with uncertainty in parentheses, followed by calculated values in parentheses. <sup>g</sup>)  $\Delta_f U^o$  = experimentally determined (back-calculated from  $\Delta_c U^o$ ) energy of formation with uncertainty in parentheses, followed by calculated values in parentheses. <sup>h</sup>)  $\Delta_f H^o$  = experimentally determined enthalpy of formation with uncertainty in parentheses, followed by calculated values in parentheses.

maximum setting in the friction tester ( $> 360 \text{ N}$ )<sup>4</sup>) [33][34]. The N-rich salts **1–4** containing the HBT<sup>2–</sup> anion were less sensitive to friction and impact than RDX or HMX (both; friction 120 N and impact 7.4 J) and TNT (friction 355 N and impact 15 J) [35]. This is to be expected because extensive H-bonding helps to stabilize a material [8][9], and is interesting since the two tunable properties of which the performance of a material is proportional, the density and heat of formation, are generally increased and only slightly decreased (less positive), respectively [2b]. Since the performance of an energetic material is most heavily dependent on density, increases in this property tend to outweigh the adverse affect on heat of formation caused by strong H-bonding [35]. This is the principal reason why compounds that can form multiple H-bonds are of interest as prospective insensitive materials with high densities and performances [9][36]. Lastly, all N-rich 5,5'-(hydrazine-1,2-diyl)bis[1*H*-tetrazol-1-ide] salts reported here are safe for transport under the UN Recommendations on the Transport of Dangerous Goods<sup>4</sup>).

According to the physical and chemical properties of the N-rich 5,5'-(hydrazine-1,2-diyl)bis[1*H*-tetrazol-1-ide] derivatives **1–4** tabulated in Table 6, all salts have high N-contents, in the range between 70.6% (**1**) and 84.4% (**2**), and, as expected for N-rich compounds, highly negative O-balances<sup>5</sup>) between –60.4% (**1**) and –102.8% (**4**)

<sup>4</sup>) Impact: insensitive  $> 40 \text{ J}$ , less sensitive  $\geq 35 \text{ J}$ , sensitive  $\geq 4 \text{ J}$ , and very sensitive  $\leq 3 \text{ J}$ . Friction: insensitive  $> 360 \text{ N}$ , less sensitive  $= 360 \text{ N}$ , sensitive  $< 360 \text{ N}$  and  $> 80 \text{ N}$ , very sensitive  $\leq 80 \text{ N}$ , and extremely sensitive  $\leq 10 \text{ N}$ . According to the UN Recommendations on the Transport of Dangerous Goods, (+) indicates: not safe for transport.

<sup>5</sup>) Calculation of the O-balance:  $\Omega [\%] = (O - 2C - H/2) 1600/M$ ; *O* = number of O-atoms, *C* = number of C-atoms, *H* = number of H-atoms, and *M* = molecular mass.

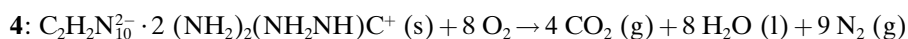
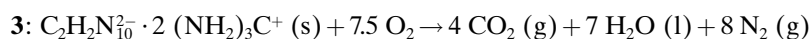
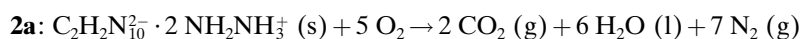
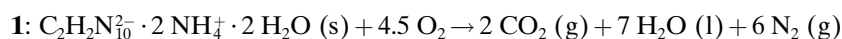
Table 7. Initial Safety Testing Results and Calculated Energetic Performance of N-Rich Salts of 5,5'-(Hydrazine-1,2-diyl)bis[1H-tetrazole] (HBT) (by using the EXPLO5 code) and Comparison with Analogous Salts of BTA and H<sub>2</sub>ZT<sup>a</sup>)

	$T_{\text{ex}}$ [K] <sup>b</sup>	$V_0$ [L kg <sup>-1</sup> ] <sup>c</sup>	$P$ [Gpa] <sup>d</sup>	$D$ [m s <sup>-1</sup> ] <sup>e</sup>	Impact [J] <sup>f</sup>	Friction [N] <sup>f</sup>	ESD (+/-) <sup>g</sup>	Thermal shock
<b>1</b>	2938 (3849)	962 (960)	31.3 (39.4)	9423 (10330)	> 30	> 360	–	deflagrates
<b>2</b>	2756 (3819)	935 (929)	29.0 (38.5)	9272 (10341)	> 30	> 360	–	deflagrates
<b>3</b>	1880 (2928)	876 (870)	19.9 (29.2)	7914 (9159)	> 30	> 360	–	deflagrates
<b>4</b>	2240 (3124)	893 (888)	24.6 (33.1)	8630 (9666)	> 30	> 360	–	deflagrates
ABTA <sup>h</sup> )			(21.6)	(8309)				
HBTA <sup>h</sup> )			(34.9)	(9926)				
GBTA <sup>h</sup> )			(17.5)	(7636)				
AGBTA <sup>h</sup> )			(22.9)	(8486)				
DAGBTA <sup>h</sup> )			(23.6)	(8560)				
TAGBTA <sup>h</sup> )			(23.9)	(8572)				
GZT <sup>i</sup> )	(3154)	975 (843)	15.4 (26.0)	6192 (8682)	32	> 360		burns
AGZT <sup>i</sup> )	(3321)	999 (865)	16.6 (28.1)	6418 (8994)	15	> 360		deflagrates
DAGZT <sup>i</sup> )	(3432)	1026 (881)	20.4 (33.0)	7045 (9601)	4	> 360		deflagrates
TAGZT <sup>i</sup> )	(3644)	1058 (895)	24.2 (35.3)	7654 (9902)	4	60		deflagrates

<sup>a</sup>) Calculated values in parentheses. <sup>b</sup>)  $T_{\text{ex}}$  = temperature of the explosion gases. <sup>c</sup>)  $V_0$  = volume of the explosion gases. <sup>d</sup>)  $P$  = detonation pressure. <sup>e</sup>)  $D$  = detonation velocity. <sup>f</sup>) Impact and friction sensitivities; tests according to BAM methods<sup>4</sup>) [9][35]. <sup>g</sup>) Rough sensitivity to the electrostatic discharge (ESD) of a Tesla coil (ca. 20 kV, HF-vacuum-tester type VP 24): + sensitive, – insensitive. <sup>h</sup>) Only the detonation parameters ( $P$  and  $D$ ) obtained by using the CHEETAH software are reported for the salts of BTA [21]. BTA salts: A (ammonium), H (hydrazinium), G (guanidinium), AG (aminoguanidinium), DAG (diaminoguanidinium), and TAG (triaminoguanidinium). <sup>i</sup>) The detonation parameters for the salts of H<sub>2</sub>ZT are based on Kamlet and Jacobs equations, and the gas volume was predicted with the ICT code [28]. H<sub>2</sub>ZT salts: G (guanidinium), AG (aminoguanidinium), DAG (diaminoguanidinium), and TAG (triaminoguanidinium).

similar to TNT ( $\Omega = -74.0\%$ ). The densities, from X-ray or picnometer measurements, are higher than those of analogous 5,5'-azobis[1H-tetrazol-1-ide] salts [20] and comparable to those of the recently reported BTA salts by Shreeve and co-workers with the same cations [21]. These density values play a determining role in the values for the detonation parameters of the compounds (see discussion below).

The energies of formation of the N-rich derivatives of HBT were back-calculated from the heat of combustion on the basis of their combustion equations (see below), Hess's law, the known standard heats of formation for H<sub>2</sub>O and CO<sub>2</sub> [37], and a correction for change in gas volume during combustion. The experimentally determined values for all materials are highly positive, and their heats of formation are in some instances comparable to that of bishydrazinium 5,5'-azobis[1H-tetrazol-1-ide] [38].



With the molecular formula, the energy of formation, and either the calculated (from X-ray) or measured (from picnometer) density, the EXPLO5 code [39] was used to calculate the detonation parameters of the N-rich salts **1–4** of HBT. The results are summarized in *Table 7*, together with the detonation parameters of some BTA salts for comparison purposes, *i.e.*, the ammonium (ABTA), hydrazinium (HBTA), guanidinium (GBTA), aminoguanidinium (AGBTA), diaminoguanidinium (DAGBTA), and triaminoguanidinium salts (TAGBTA). The values presented in *Table 7* for the detonation parameters of salts of BTA are all predicted based on isodesmic reactions [21] to calculate the heats of formation of the compounds and by means of the CHEETAH software [40].

Formation of the N-rich salts **1–4** containing the  $\text{HBT}^{2-}$  anion results in compounds which are much less sensitive towards friction and impact [11][41] than the free acid HBT [6][13], while still having high (calculated based on the MP2 method) detonation pressures and velocities above *ca.* 30 GPa and *ca.* 9000 m s<sup>-1</sup>, respectively (*Table 7*). The decrease of the predicted performance when comparing HBT with its N-rich salts is expected due to the lower density of the salts. This is a similar observation to that made for N-rich salts of 5-[(5-nitro-1*H*-tetrazol-2-yl)methyl]-1*H*-tetrazole [42], where the free acid is also relatively sensitive (towards impact), but formation of N-rich salts results in a slight decrease of the detonation parameters and the formation of insensitive (or less sensitive) materials. Furthermore, the (EXPLO5) detonation parameters of HBT and its salts fit nicely with and are higher than the calculated values for salts of BTA (CHEETAH) [21] or those containing the  $\text{ZT}^{2-}$  anion (EXPLO5) [20c] and the same N-rich cations (*i.e.*, guanidinium (GZT), aminoguanidinium (AGZT), diaminoguanidinium (DAGZT), and triaminoguanidinium (TAGZT)). Lastly, it is important to point out that the systematic overestimation of the detonation parameters based on electronic energies is specially high when comparing the (MP2 method) computed values for 5,5'-azobis[1*H*-tetrazol-1-ide] salts with those predicted by the *Kamlet* and *Jacobs* equations (*Table 7*), in particular when dealing with compounds which form extensive strong H-bonds in the solid state. Therefore, we believe the disagreement between computed and 'experimental' detonation parameters for the 5,5'-(hydrazine-1,2-diyl)bis[1*H*-tetrazole] derivatives studied here to be justified.

Although neutral 5,5'-(hydrazine-1,2-diyl)bis[1*H*-tetrazole] (HBT) is a solid which is perfectly stable towards oxidation when left in contact with air for extended periods of time [13], the N-rich salts **1–4** containing the  $\text{HBT}^{2-}$  anion might see their application limited, regardless of their interesting energetic properties, due to slow oxidation when left in contact with air. The salts **1** and **3** turn yellow (oxidation to the 5,5'-azobis[1*H*-tetrazol-1-ide] derivative) on standing in air for several days in an open beaker, whereas **2** and **4** contain both a (reducing) hydrazine moiety which prevents

oxidation, and the materials are stable for at least several months when stored in closed containers. A way of taking advantage of the energetic properties of these compounds, regardless of their susceptibility to oxidation, would certainly prove useful. For example, it might be suggested to sacrifice some of the performance of these materials by coating them (*e.g.*, wax) or mixing them with a reducing agent (*e.g.*, finely divided magnesium powder), depending on the application, making them more stable towards oxidation.

Due to the negative O-balances of all materials studied here, it is of interest to calculate mixtures with an oxidizer at a neutral O-balance to further increase the performance in comparison with the pure compounds. Thus, the detonation parameters for formulations of all 5,5'-(hydrazine-1,2-diyl)bis[1*H*-tetrazole] derivatives with an oxidizer such as ammonium nitrate (AN) or ammonium dinitramide (ADN) were calculated (*Tables 8 and 9*). The detonation parameters of the high-performing salts **1–4** are only decreased by adding an oxidizer, much more notoriously in the case of mixtures with AN. In summary, the relatively well ‘O-balanced’ N-rich compounds **1–4** are already outstandingly high-performing as the pure materials, and formulations with an oxidizer do not do but decrease the performance values.

Table 8. *Thermodynamic and Explosive Properties of Formulations of N-Rich 5,5'-(Hydrazine-1,2-diyl)bis[1H-tetrazol-1-ide] Salts with Ammonium Nitrate (AN)*

	AN/ <b>1</b> <sup>a)</sup>	AN/ <b>2</b> <sup>b)</sup>	AN/ <b>3</b> <sup>c)</sup>	AN/ <b>4</b> <sup>d)</sup>
$\rho$ [g cm <sup>-3</sup> ] <sup>e)</sup>	1.697	1.693	1.699	1.701
Average $M_r$	119.56	115.03	119.19	127.25
$\Omega$ [%] <sup>f)</sup>	-0.1	-0.5	+0.2	-0.2
$\Delta U_f^\circ$ [kJ kg <sup>-1</sup> ] <sup>g)</sup>	-2809	-2658	-3326	-3117
$\Delta H_f^\circ$ [kJ kg <sup>-1</sup> ] <sup>h)</sup>	-2951	-2802	-3464	-3258
$T_{ex}$ [K] <sup>i)</sup>	3097	3020	2832	2906
$V_0$ [l kg <sup>-1</sup> ] <sup>j)</sup>	982	979	964	969
$P$ [GPa] <sup>k)</sup>	27.1	25.7	24.3	25.0
$D$ [m s <sup>-1</sup> ] <sup>l)</sup>	8420	8236	8022	8117

a) 75% AN + 25% **1**. b) 77% AN + 23% **2**. c) 81% AN + 19% **3**. d) 80% AN + 20% **4**. e)  $\rho$  = density from EXPLO5. f)  $\Omega$  = O-balance. g)  $\Delta U_f^\circ$  = calculated energy of formation. h)  $\Delta H_f^\circ$  = calculated enthalpy of formation. i)  $T_{ex}$  = temperature of the explosion gases. j)  $V_0$  = volume of the explosion gases. k)  $P$  = detonation pressure. l)  $D$  = detonation velocity.

3.5. *Decomposition Gases of Salts of HBT*. Predictions about the gases formed upon decomposition and the heats of explosions of the N-rich salts **1–4** of HBT were done with the ICT computer program [44]. The molecular formulas, calculated (from X-ray) or experimentally determined (from picnometer measurements) and the experimentally determined (back-calculated from the bomb calorimetry results) molar heats of combustion were used for the calculations. *Table 10* contains the results of these calculations as well as those for commonly used energetic materials for the sake of comparison. Fig. 2 of the supplementary material<sup>3)</sup> contains graphical representations of the results presented in *Table 10*.

As can be read from *Table 10*, the heats of explosion of the N-richer ammonium and hydrazinium salts **1** and **2**, respectively, are comparable to that of the commonly used

Table 9. *Thermodynamic and Explosive Properties of Formulations of N-Rich 5,5'-(Hydrazine-1,2-diyl)bis[1H-tetrazol-1-ide] Salts with Ammonium Dinitramide (ADN)*

	ADN/1 <sup>a)</sup>	ADN/2 <sup>b)</sup>	ADN/3 <sup>c)</sup>	ADN/4 <sup>d)</sup>
$\rho$ [g cm <sup>-3</sup> ] <sup>e)</sup>	1.752	1.751	1.759	1.762
Average $M_r$	158.30	153.26	162.97	170.18
$\Omega$ [%] <sup>f)</sup>	-0.1	+0.2	-0.5	+0.2
$\Delta U_f^\circ$ [kJ kg <sup>-1</sup> ] <sup>g)</sup>	-150	86	-501	-321
$\Delta H_f^\circ$ [kJ kg <sup>-1</sup> ] <sup>h)</sup>	-293	-59	-640	-461
$T_{ex}$ [K] <sup>i)</sup>	3917	3908	3730	3801
$V_0$ [l kg <sup>-1</sup> ] <sup>j)</sup>	930	921	906	909
$P$ [Gpa] <sup>k)</sup>	33.1	32.6	31.4	31.9
$D$ [m s <sup>-1</sup> ] <sup>l)</sup>	9038	8978	8830	8891

<sup>a)</sup> 70% ADN + 30% **1**. <sup>b)</sup> 73% ADN + 27% **2**. <sup>c)</sup> 76% ADN + 24% **3**. <sup>d)</sup> 76% ADN + 24% **4**. <sup>e)</sup>  $\rho$  = density from EXPLO5. <sup>f)</sup>  $\Omega$  = O-balance. <sup>g)</sup>  $\Delta U_f^\circ$  = calculated energy of formation. <sup>h)</sup>  $\Delta H_f^\circ$  = calculated enthalpy of formation. <sup>i)</sup>  $T_{ex}$  = temperature of the explosion gases. <sup>j)</sup>  $V_0$  = volume of the explosion gases. <sup>k)</sup>  $P$  = detonation pressure. <sup>l)</sup>  $D$  = detonation velocity.

Table 10. *Predicted Decomposition Gases and Heats of Explosion of N-Rich Salts of HBT and Comparison with Known High Explosives (by using the ICT code)<sup>a)</sup>*

	CO <sub>2</sub>	H <sub>2</sub> O	N <sub>2</sub>	CO	H <sub>2</sub>	NH <sub>3</sub>	CH <sub>4</sub>	HCN	C	$\Delta H_{ex}$ [cal g <sup>-1</sup> ] <sup>b)</sup>
<b>1</b>	0.8	149.9	525.3	1.0	1.8	218.4	7.5	1.3	94.0	1658
<b>2</b>	- <sup>c)</sup>	- <sup>c)</sup>	628.2	- <sup>c)</sup>	2.1	262.1	13.4	1.4	92.8	1512
<b>3</b>	- <sup>c)</sup>	- <sup>c)</sup>	589.3	- <sup>c)</sup>	2.5	234.6	20.1	1.3	152.2	1003
<b>4</b>	- <sup>c)</sup>	- <sup>c)</sup>	591.5	- <sup>c)</sup>	2.4	249.2	17.2	1.3	138.4	1112
RDX <sup>d)</sup>	292.6	232.8	373.9	21.5	0.2	5.1	- <sup>c)</sup>	0.3	72.7	1593
TEX <sup>e)</sup>	405.4	199.8	211.4	27.5	0.2	0.3	- <sup>c)</sup>	- <sup>c)</sup>	152.2	1237

<sup>a)</sup> The amount of gases formed at 298 K is given in g of gas per kg of energetic compound. <sup>b)</sup>  $\Delta H_{ex}$  = heat of explosion. <sup>c)</sup> - means that this gas was not predicted by the ICT code. <sup>d)</sup> RDX = hexahydro-1,3,5-trinitro-1,3,5-triazine. <sup>e)</sup> TEX = hexahydro-4,7-dinitro-5,2,6-(epoxymethenoxy)-1,3-dioxolo[4,5-*b*]pyrazine = 4,10-dinitro-2,6,8,12-tetraoxa-4,10-diazatetracyclo[5.5.0.0<sup>3,11</sup>.0<sup>5,9</sup>]dodecane.

RDX, whereas those of the guanidinium salts **3** and **4** are slightly below that of TEX. The amounts of carbon soot predicted by the code are as expected higher for **3** and **4** and in any case below the amounts expected from the decomposition of TEX. On the other hand, the amounts of N<sub>2</sub> expected from the decomposition of salts **1–4** are almost twice as large as that predicted for commonly used energetic compounds, which is in agreement with the logic that N-rich compounds owe their high energy content to the formation of molecular N<sub>2</sub> [45]. The anticipated amounts of highly toxic gases (*i.e.*, HCN and CO) is low or null for all materials, whereas the expected amounts of NH<sub>3</sub> are much larger for compounds **1–4** than for RDX and TEX, as expected due to the presence of NH moieties in the former salts. Lastly, H<sub>2</sub> and CH<sub>4</sub> are predicted to be formed in relatively small amounts.

**4. Conclusions.** – The 5,5'-(hydrazine-1,2-diyl)bis[1H-tetrazole] (HBT) is a prospective candidate for applications in gas generators, propellants, or additives in

solid rockets as low-smoke propellant ingredients. The moderate friction-sensitivity value of HBT (108 N) could be reduced by forming several N-rich salts with ammonium, hydrazinium, and guanidinium cations (compounds **1–4**). The salts **1–4** have high detonation parameters and are yet insensitive materials; however, they oxidize slowly to the 5,5'-azobis[1*H*-tetrazol-1-ide] salts over time, which limits their range of application. This might be overcome either by coating the material with wax or by using a reducing agent (e.g., Mg powder), depending on the application. Efforts in this direction are currently being undertaken. The crystal structure of the ammonium salt **1** was discussed in detail as a representative example of a salt containing the HBT<sup>2-</sup> anion. Lastly, the energetic properties of all materials were analyzed in detail and suggest potential for application as environment friendly, highly energetic materials.

### Experimental Part

**Caution!** Although we had no difficulties handling the compounds described here, 1*H*-tetrazoles and their derivatives are nevertheless energetic materials, and the explosive properties of the compounds described herein are not well-established. We recommend the syntheses to be carried out only by expert personnel, wearing protective gear (i.e., Kevlar gloves, wrist protectors, leather jacket, helmet, ear plugs...) and using conductive equipment, specially when working on a larger scale.

**General.** All reagents and solvents were obtained from Sigma–Aldrich Inc. or Acros Organics (anal. grade) and were used as supplied. M.p.: by differential-scanning calorimetry (Linseis-DSC-PT-10 instrument [46] calibrated with standard pure indium and zinc); heating rate 5° min<sup>-1</sup>; in closed aluminium sample pans with a 1 µm hole in the top for gas release under an N<sub>2</sub> flow of 20 ml min<sup>-1</sup>, with an empty identical aluminium sample pan as a reference. IR Spectra: Perkin-Elmer-Spectrum-One FT-IR instrument; KBr pellets at 20° [47];  $\tilde{\nu}$  in cm<sup>-1</sup>. Raman Spectra: Perkin-Elmer-Spectrum-2000R-NIR FT-Raman instrument equipped with a Nd:YAG laser (1064 nm);  $\tilde{\nu}$  in cm<sup>-1</sup> and intensities in % of the most intense peak in parentheses. <sup>1</sup>H-, <sup>13</sup>C-, and <sup>15</sup>N-NMR Spectra: Jeol-Eclipse-400; instrument, in (D<sub>6</sub>)DMSO at or near 25°; chemical shifts  $\delta$  in ppm rel. to Me<sub>4</sub>Si (<sup>1</sup>H, <sup>13</sup>C) as external standard and coupling constants *J* in Hz. Elemental analyses: Netsch-STA 429 simultaneous thermal analyzer.

**X-Ray Crystallography.** The structures of **1** and **5** were determined by X-ray analysis with an Oxford Xcalibur3 diffractometer, a Spellman generator (voltage 50 kV, current 40 mA) and a KappaCCD detector. Suitable crystals were obtained as described below. The data collections were performed with the CrysAlis CCD software [48], and the data reduction with the CrysAlis RED software [49]. The structures were solved by direct methods with the standard software implemented in the WinGX package [50–53] and finally checked with the PLATON software [54]. All non-H-atoms were refined anisotropically. All H-atoms were located from difference Fourier electron-density maps and refined isotropically. The absorptions were corrected with the SCALE3 ABSPACK multi-scan method [55]. Further information concerning the crystal-structure determination (excluding structure factors) is available from the Cambridge Crystallographic Data Centre<sup>6)</sup>.

**Bomb Calorimetry.** For the calorimetric measurements of the 5,5'-(hydrazine-1,2-diyl)bis[1*H*-tetrazol-1-ide] salts, a Parr-1356 bomb calorimeter (static jacket) equipped with a Parr-207A O<sub>2</sub> bomb for the combustion of highly energetic materials was used [56]. A Parr-1755 printer, furnished with the Parr-1356 calorimeter, was used to produce a permanent record of all activities within the calorimeter. The samples (ca. 200 mg each) were carefully mixed with anal.-grade benzoic acid (ca. 800 mg) and carefully pressed into pellets, which were subsequently burned in a 3.05 MPa atmosphere of pure O<sub>2</sub>. The experimentally determined constant-volume energies of combustion ( $\Delta_c U_{\text{exp}}$ ) were obtained as the averages of three to five single measurements with standard deviations calculated as a measure of exper.

<sup>6)</sup> CCDC-705173 and -705174 contain the supplementary crystallographic data for **1** and **5**. These data can be obtained free of charge via [http://www.ccdc.cam.ac.uk/data\\_request/cif](http://www.ccdc.cam.ac.uk/data_request/cif).



uncertainty. The calorimeter was calibrated by the combustion of certified benzoic acid in an O<sub>2</sub> atmosphere at a pressure of 3.05 MPa.

*Computational Details.* The EXPLO5 software with the following values for the empirical constants in the Becker–Kistiakowsky–Wilson equation of state was used:  $\alpha = 0.5$ ,  $\beta = 0.176$ ,  $\kappa = 14.71$ , and  $\theta = 6620$ . To correlate the measured values for the physical and chemical properties and detonation parameters of the compounds, density-functional theory (DFT) calculations were carried out with the program package G03W [57]. For the ionic compounds, the electronic energies for all cations and the 5,5'-(hydrazine-1,2-diyl)bis[1H-tetrazol-1-ide] anion were calculated by the Møller–Plesset perturbation theory truncated at the second order (MP2) [58] and were used unscaled. The results of the MP2 electronic-energy calculations are tabulated in Table 1 the supplementary material<sup>3</sup>. For all atoms in all calculations, the Dunning's correlation consistent polarized double-zeta basis set cc-pVDZ was used [59][60]. The exper. and calc. values for the ionic salts **1–4** based on the MP2 method are given in Table 6.

*5,5'-(Hydrazine-1,2-diyl)bis[1H-tetrazole]* (HBT). HBT was synthesized from sodium 5,5'-azo-bis[1H-tetrazol-1-ide] [24], magnesium, and hydrochloric acid in 93% yield according to our previously published procedure [6]. DSC (5° min<sup>-1</sup>): 207° (dec.). Anal. calc. for C<sub>2</sub>H<sub>14</sub>N<sub>12</sub>O<sub>2</sub> (168.12): C 14.28, H 2.40, N 83.31; found: C 14.17, H 2.29, N 82.94.

*Diammonium 5,5'-(Hydrazine-1,2-diyl)bis[1H-tetrazol-1-ide] Dihydrate* (= 5,5'-(Hydrazine-1,2-diyl)bis[2H-tetrazole] Ion(2–) Ammonium Salt Hydrate (1:2:2); **1**). A 25% NH<sub>3</sub> soln. (40 ml) in a Schlenk flask was purged N<sub>2</sub> to displace the O<sub>2</sub> in soln. HBT (2.079 g, 12.4 mmol) was added slowly keeping a flow of N<sub>2</sub>, and the mixture was left to react for 15 min (→ clear colorless soln.). The solvent was then carefully removed by slow evaporation under N<sub>2</sub>: pure **1** (2.854 g, 97%). This procedure yielded some single crystals of **1** suitable for X-ray analysis. DSC (5° min<sup>-1</sup>): ca. 111° (–H<sub>2</sub>O), 196° (dec.). IR (KBr): 3129m, 2995m, 1699w, 1626w, 1553m, 1483m, 1426vs, 1376s, 1226m, 1206m, 1152w, 1138m, 1120m, 1075m, 1024m, 997s, 938m, 791s, 727s, 611s, 582s. Raman (400 mW, 25°): 3137 (11), 1714 (3), 1521 (25), 1487 (8), 1418 (6), 1402 (8), 1379 (5), 1246 (4), 1227 (18), 1208 (17), 1153 (5), 1140 (6), 1124 (20), 1074 (48), 1018 (9), 941 (5), 726 (4), 397 (9), 349 (10), 235 (19), 188 (18). <sup>1</sup>H-NMR ((D<sub>6</sub>)DMSO): 7.8 (s, NHNH); 5.5 (s, 2 NH<sub>4</sub><sup>+</sup>). <sup>13</sup>C-NMR ((D<sub>6</sub>)DMSO): 164.7 (2 C<sub>ring</sub>). FAB-MS (neg., Xe, 6 keV, glycerol matrix): 167.0 (100, C<sub>2</sub>H<sub>3</sub>N<sub>10</sub><sup>-</sup>), 335.0 (68, C<sub>2</sub>H<sub>4</sub>N<sub>10</sub>·C<sub>2</sub>H<sub>3</sub>N<sub>10</sub><sup>-</sup>). FAB-MS (pos., Xe, 6 keV, glycerol matrix): 18.0 (3, NH<sub>4</sub><sup>+</sup>). Anal. calc. for C<sub>2</sub>H<sub>14</sub>N<sub>12</sub>O<sub>2</sub> (238.14): C 10.08, H 5.92, N 70.56; found: C 10.21, H 5.83, N 70.54.

*Bis(hydrazinium) 5,5'-(Hydrazine-1,2-diyl)bis[1H-tetrazol-1-ide]* (= 5,5'-(Hydrazine-1,2-diyl)bis[2H-tetrazole] Ion(2–) Hydrazinium Salt (1:2); **2a**). A Schlenk flask was loaded with dist. H<sub>2</sub>O (20 ml), which had been freed of O<sub>2</sub> by flushing with N<sub>2</sub> gas through the soln. for 10 min. A soln. of 24% aq. hydrazine (5.34 g, 40.0 mmol) was added, and then HBT (1.681 g, 10.0 mmol) portionwise under a stream of N<sub>2</sub>. The mixture was stirred for 30 min at r.t. and the solvent evaporated under high vacuum: pure **2a** (91%). DSC (5° min<sup>-1</sup>): ca. 154–182° (m.p., dec.). IR (KBr): 3269m, 3162w, 2971w, 2836m, 2703 m, 2612m, 2139vw, 1650vw, 1615m, 1552m, 1523s, 1467s, 1416m, 1360s, 1271vw, 1222m, 1100vs, 1061m, 1013m, 959s, 809m, 758m, 717m, 598s, 592s, 568s. Raman (400 mW, 25°): 3169 (7), 1645 (9), 1549 (17), 1515 (24), 1478 (12), 1411 (12), 1388 (21), 1366 (15), 1231 (35), 1118 (19), 1056 (100), 1009 (20), 961 (26), 815 (13), 748 (11), 412 (10), 230 (23). <sup>1</sup>H-NMR ((D<sub>6</sub>)DMSO): 8.0 (s, NHNH); 5.9 (s, ca. 10 H, H<sub>2</sub>NNH<sub>3</sub><sup>+</sup>). <sup>13</sup>C-NMR ((D<sub>6</sub>)DMSO): 167.4 (2 C<sub>ring</sub>). FAB-MS (neg., Xe, 6 keV, glycerol matrix): 84.0 (12, CH<sub>2</sub>N<sub>5</sub><sup>-</sup>), 118.1 (3, HCN·gly<sup>-</sup>), 124.1 (3, C<sub>2</sub>H<sub>2</sub>N<sub>7</sub><sup>-</sup>), 166.0 (17, C<sub>2</sub>H<sub>2</sub>N<sub>10</sub><sup>-</sup>), 167.0 (100, C<sub>2</sub>H<sub>3</sub>N<sub>10</sub><sup>-</sup>), 259.1 (12, C<sub>2</sub>H<sub>4</sub>N<sub>10</sub>·gly<sup>-</sup>), 335.0 (46, C<sub>2</sub>H<sub>4</sub>N<sub>10</sub>·C<sub>2</sub>H<sub>3</sub>N<sub>10</sub><sup>-</sup>). FAB-MS (pos., Xe, 6 keV, glycerol matrix): 33.1 (9, N<sub>2</sub>H<sub>5</sub><sup>+</sup>). Anal. calc. for C<sub>2</sub>H<sub>12</sub>N<sub>14</sub> (232.14): C 10.34, H 5.21, N 84.45; found: C 10.33, H 5.11, N 83.93.

*Bis(hydrazinium) 5,5'-(Hydrazine-1,2-diyl)bis[1H-tetrazol-1-ide] Monohydrate* (= 5,5'-(Hydrazine-1,2-diyl)bis[2H-tetrazole] Ion(2–) Hydrazinium Salt Compd. with Hydrazine (1:2:1); **2**). As described for **2a** on a 20 mmol scale with 99% hydrazine hydrate as the solvent for the reaction: **2** (100%). DSC (5° min<sup>-1</sup>): 186° (m.p., dec.). IR (KBr): 3292s, 3171m, 2985m, 2857m, 2708m, 2618m, 2139w, 1617s, 1556s, 1529vs, 1469s, 1417w, 1361s, 1223w, 1112vs, 1013w, 960s, 814w, 759w, 717w, 573m. Raman (400 mW, 25°): 3276 (4), 3187 (7), 1624 (6), 1506 (18), 1373 (11), 1214 (17), 1202 (14), 1141 (9), 1119 (10), 1061 (100), 1012 (2), 957 (11), 818 (3), 614 (9), 421 (6), 374 (4), 230 (16). <sup>1</sup>H-NMR ((D<sub>6</sub>)DMSO): 7.41 (s, NHNH); 5.34 (s, ca. 14 H, H<sub>2</sub>NNH<sub>2</sub>, H<sub>2</sub>NNH<sub>3</sub><sup>+</sup>). <sup>13</sup>C-NMR ((D<sub>6</sub>)DMSO): 166.4

(2 C<sub>ring</sub>). FAB-MS (neg., Xe, 6 keV, glycerol matrix): 84.0 (8, CH<sub>2</sub>N<sub>5</sub><sup>-</sup>), 118.1 (4, HCN·gly<sup>-</sup>), 124.1 (1, C<sub>2</sub>H<sub>2</sub>N<sub>7</sub><sup>-</sup>), 166.0 (12, C<sub>2</sub>H<sub>2</sub>N<sub>10</sub><sup>-</sup>), 167.0 (100, C<sub>2</sub>H<sub>3</sub>N<sub>10</sub><sup>-</sup>), 259.1 (7, C<sub>2</sub>H<sub>4</sub>N<sub>10</sub>·gly<sup>-</sup>), 335.0 (28, C<sub>2</sub>H<sub>4</sub>N<sub>10</sub>·C<sub>2</sub>H<sub>3</sub>N<sub>10</sub><sup>-</sup>). Anal. calc. for C<sub>2</sub>H<sub>16</sub>N<sub>16</sub> (264.25): C 9.09, H 6.10, N 84.81; found: C 9.27, H 6.06, N 84.74.

*Guanidinium 5,5'-(Hydrazine-1,2-diyl)bis[1H-tetrazolate-1-ide]* (= Guanidinium Salt with 5,5'-(Hydrazin-1,2-diyl)bis[2H-tetrazole] (2:1); **3**). H<sub>2</sub>O (20 ml) in a Schlenk flask was degassed by flushing with N<sub>2</sub> for 10 min. Guanidinium carbonate (0.629 g, 3.5 mmol) and HBT (0.587 g, 3.5 mmol) were suspended in H<sub>2</sub>O, and the mixture was stirred for 30 min at r.t. under a stream of N<sub>2</sub> with concomitant gas evolution (CO<sub>2</sub>). The formed clear colorless soln. was heated to 60° and concentrated under high vacuum: **3** (0.980 g, 98%). Slightly yellow solid. DSC (5° min<sup>-1</sup>): 214° (dec.). IR (KBr): 3336w, 3153m, 1650s, 1585w, 1548w, 1466m, 1399vw, 1365m, 1270vw, 1240vw, 1216vw, 1087vs, 1015m, 961w, 747m, 737m, 617s, 606s, 578s. Raman (400 mW, 25°): 3259 (6), 1523 (27), 1360 (7), 1227 (16), 1214 (18), 1162 (8), 1125 (17), 1060 (59), 1009 (77), 860 (10), 735 (10), 549 (23), 517 (15), 375 (13), 332 (12), 203 (13). <sup>1</sup>H-NMR ((D<sub>6</sub>)DMSO): 7.1 (s, 8 H, C=NH<sub>2</sub><sup>+</sup>, HNNH). <sup>13</sup>C-NMR ((D<sub>6</sub>)DMSO): 157.8 (C=NH<sub>2</sub><sup>+</sup>), 167.9 (2 C<sub>ring</sub>). FAB-MS (neg., Xe, 6 keV, glycerol matrix): 84.0 (4, CH<sub>2</sub>N<sub>5</sub><sup>-</sup>), 118.1 (3, HCN·gly<sup>-</sup>), 166.0 (12, C<sub>2</sub>H<sub>2</sub>N<sub>10</sub><sup>-</sup>), 167.0 (100, C<sub>2</sub>H<sub>3</sub>N<sub>10</sub><sup>-</sup>), 259.0 (28, C<sub>2</sub>H<sub>4</sub>N<sub>10</sub>·gly<sup>-</sup>), 335.0 (8, C<sub>2</sub>H<sub>4</sub>N<sub>10</sub>·C<sub>2</sub>H<sub>3</sub>N<sub>10</sub><sup>-</sup>). FAB-MS (pos., Xe, 6 keV, glycerol matrix): 60.2 (7, CH<sub>6</sub>N<sub>3</sub><sup>+</sup>). Anal. calc. for C<sub>4</sub>H<sub>14</sub>N<sub>16</sub> (268.16): C 16.77, H 4.93, N 78.30; found: C 16.48, H 4.98, N 77.75.

*Aminoguanidinium 5,5'-(Hydrazine-1,2-diyl)bis[1H-tetrazol-1-ide]* (= N''-Aminoguanidinium Salt with 5,5'-(Hydrazine-1,2-diyl)bis[2H-tetrazole]; **4**). In a Schlenk flask, H<sub>2</sub>O (20 ml) was degassed by flushing with N<sub>2</sub> for 10 min. Aminoguanidinium hydrogen carbonate<sup>7)</sup> (0.861 g, 6.3 mmol) and HBT (0.532 g, 3.2 mmol) were added forming a suspension, which turned into a clear soln. after stirring for 30 min at r.t. (gas evolution!). The solvent was evaporated under high vacuum in a warm H<sub>2</sub>O bath: pure **4** (0.985 g, 97%). As an off-yellow solid. Slow evaporation of an aq. soln. of the salt under a flow of N<sub>2</sub> led to the formation of **4** as a powder and a small amount of single crystals of a by-product, which was identified as betaine **5**<sup>7)</sup> by X-ray measurements. **4**: DSC (5° min<sup>-1</sup>): ca. 142–194° (m.p., dec.). IR (KBr): 3327m, 3269m, 3165m, 3046m, 2787vw, 2231vw, 2206vw, 2094vw, 1666s, 1645s, 1586w, 1457m, 1397m, 1240vw, 1203w, 1177w, 1164w, 1110m, 1077w, 1054w, 1037w, 1007m, 769m, 738vs, 632s, 616s. Raman (400 mW, 25°): 3231 (8), 1652 (11), 1574 (13), 1512 (53), 1233 (40), 1105 (23), 1048 (100), 956 (37), 820 (13), 616 (15), 537 (14), 513 (27), 406 (13), 373 (35), 336 (15), 225 (36). <sup>1</sup>H-NMR ((D<sub>6</sub>)DMSO): 7.7 (s, 4 H, C=NH<sub>2</sub><sup>+</sup>, NHH), 7.1 (s, NH), 4.8 (s, NH<sub>2</sub>). <sup>13</sup>C-NMR ((D<sub>6</sub>)DMSO): 158.6 (C=NH<sub>2</sub><sup>+</sup>), 159.5 (2 C<sub>ring</sub>). FAB-MS (neg., Xe, 6 keV, glycerol matrix): 167.0 (42, C<sub>2</sub>H<sub>3</sub>N<sub>10</sub><sup>-</sup>). FAB-MS (pos., Xe, 6 keV, glycerol matrix): 75.1 (35, CH<sub>7</sub>N<sub>4</sub><sup>+</sup>). Anal. calc. for C<sub>4</sub>H<sub>16</sub>N<sub>18</sub> (316.18): C 15.18, H 5.10, N 79.72; found: C 15.24, H 5.11, N 78.90.

## REFERENCES

- [1] K. Redecker, W. Weuter, U. Bley, D. Schmittner, to *Dynamit Nobel AG*, Ger. Pat. 19730873, 1998; Y.-L. Peng, C.-W. Wong, to Chung Shan Inst. of Science, U.S. Pat. 5877300, 1999.
- [2] a) A. Hammerl, T. M. Klapötke, H. Nöth, M. Warchhold, G. Holl, M. Kaiser, U. Ticmanis, *Inorg. Chem.* **2001**, *40*, 3570; b) K. Karaghiosoff, T. M. Klapötke, P. Mayer, C. Miró Sabaté, A. Penger, J. M. Welch, *Inorg. Chem.* **2008**, *47*, 1007; c) T. M. Klapötke, C. Miró Sabaté, *Heteroat. Chem.* **2008**, *19*, 301.
- [3] Y.-H. Joo, B. Twamley, S. Garg, J. M. Shreeve, *Angew. Chem., Int. Ed.* **2008**, *47*, 6236; T. Abe, G.-H. Tao, Y.-H. Joo, Y. Huang, B. Twamley, J. M. Shreeve, *Angew. Chem., Int. Ed.* **2008**, *47*, 7087.
- [4] Y.-H. Joo, J. M. Shreeve, *Org. Lett.* **2008**, *10*, 4665.
- [5] D. E. Chavez, M. A. Hiskey, R. D. Gilardi, *Angew. Chem., Int. Ed.* **2000**, *39*, 1791; V. A. Ostrovskii, M. S. Pevzner, T. P. Kofman, I. V. Tselinskii, *Targets Heterocycl. Syst.* **1999**, *3*, 467; H. Xue, H. Gao, B. Twamley, J. M. Shreeve, *Eur. J. Inorg. Chem.* **2006**, 2959.
- [6] T. M. Klapötke, C. Miró Sabaté, *Chem. Mater.* **2008**, *20*, 3629.

7) The aminoguanidinium hydrogen carbonate from *Acros* was in fact (carboxyamino)guanidine betaine monohydrate (=2-(aminoiminomethyl)hydrazinecarboxylic acid hydrate (1:1); **5**).

- [7] A. K. Sikder, N. Sikder, *J. Hazard. Mater.* **2004**, *112*, 1.
- [8] H. H. Cady, A. C. Larson, *Acta Crystallogr.* **1965**, *18*, 485.
- [9] U. Bemm, H. Östmark, *Acta Crystallogr., Sect. C* **1998**, *54*, 1997.
- [10] H. Xue, J. M. Shreeve, *Adv. Mater.* **2005**, *17*, 2142; H. Xue, B. Twamley, J. M. Shreeve, *Inorg. Chem.* **2005**, *44*, 7009.
- [11] T. M. Klapötke, P. Mayer, C. Miró Sabaté, J. M. Welch, N. Wiegand, *Inorg. Chem.* **2008**, *47*, 6014.
- [12] a) T. M. Klapötke, P. Mayer, A. Schulz, J. J. Weigand, *J. Am. Chem. Soc.* **2005**, *127*, 2032; b) M. von Denffer, T. M. Klapötke, G. Kramer, G. Spiess, J. M. Welch, G. Heeb, *Propellants, Explos., Pyrotech.* **2005**, *30*, 191; c) T. M. Klapötke, K. Karaghiosoff, P. Mayer, A. Pengler, J. M. Welch, *Propellants, Explos., Pyrotech.* **2006**, *31*, 188.
- [13] T. M. Klapötke, C. Miró Sabaté, *Z. Anorg. Allg. Chem.* **2007**, *633*, 2671.
- [14] J. Thiele, *Just. Liebigs Ann. Chem.* **1898**, *303*, 57.
- [15] R. J. Spear, P. P. Elischer, *Aust. J. Chem.* **1982**, *35*, 1.
- [16] A. Hammerl, G. Holl, T. M. Klapötke, P. Mayer, H. Nöth, H. Piotrowski, M. Warchhold, *Eur. J. Inorg. Chem.* **2002**, 834.
- [17] M. A. Hiskey, D. E. Chavez, D. L. Naud, S. F. Son, H. L. Berghout, C. A. Bolme, Proceed. 27th Inter. Pyrotech. Sem., 2000, Los Alamos, USA, p. 3; M. A. Hiskey, D. E. Chavez, D. L. Naud, to Univ. California, U.S. Pat. 6214139, 2001; S. P. Burns, J. W. Halpin, G. K. Williams, P. S. Khandhadia, D. L. Hordos, J. Newell, WO Pat. 038803, 2007; J. W. Halpin, S. P. Burns, WO Pat. 041384, 2007; T. M. Klapötke, P. Mayer, K. Polborn, J. Stierstorfer, J. J. Weigand, New Trends Res. Energ. Mater., Proceed. 9th Sem., 2006, Pardubice, Czech Republic, p. 641; M. Friedrich, J. C. Gálvez-Ruiz, T. M. Klapötke, P. Mayer, B. Weber, J. J. Weigand, *Inorg. Chem.* **2005**, *44*, 8044.
- [18] M. A. Hiskey, N. Goldman, J. R. Stine, *J. Energ. Mater.* **1998**, *16*, 119.
- [19] D. Adam, G. Holl, T. M. Klapötke, *Heteroat. Chem.* **1999**, *10*, 548; T. M. Klapötke, H.-G. Ang, *Propellants, Explos., Pyrotech.* **2001**, *26*, 221.
- [20] a) T. M. Klapötke, C. Miró Sabaté, Particles, Crystals, Composites, ICT Symp., 2007, Pfingztal, Germany; b) T. M. Klapötke, C. Miró Sabaté, *Chem. Mater.* **2008**, *20*, 1750; c) A. Hammerl, M. A. Hiskey, G. Holl, T. M. Klapötke, K. Polborn, J. Stierstorfer, J. J. Weigand, *Chem. Mater.* **2005**, *17*, 3784.
- [21] Y. Guo, H. Gao, B. Twamley, J. M. Shreeve, *Adv. Mater.* **2007**, *19*, 2884.
- [22] A. Hammerl, G. Holl, M. Kaiser, T. M. Klapötke, H. Piotrowski, *Z. Anorg. Allg. Chem.* **2003**, *629*, 2117.
- [23] G. O. Reddy, A. K. Chatterjee, *J. Hazard. Mater.* **1984**, *9*, 291; D. J. Whelan, R. J. Spear, R. W. Read, *Thermochim. Acta* **1984**, *80*, 149.
- [24] J. Thiele, *Just. Lieb. Ann. Chem.* **1892**, *270*, 1; J. Thiele, J. T. Marais, *Just. Lieb. Ann. Chem.* **1893**, *273*, 144; J. Thiele, *Ber. Dtsch. Chem. Ges.* **1893**, *26*, 2645.
- [25] T. Kolev, R. Petrova, *Acta Crystallogr., Sect. E* **2003**, *59*, o447.
- [26] T. M. Klapötke, J. Stierstorfer, unpublished results.
- [27] K. Karaghiosoff, T. M. Klapötke, C. Miró Sabaté, *Eur. J. Inorg. Chem.* **2009**, 238.
- [28] J. J. Weigand, Ph.D. Thesis, Ludwig-Maximilians Universität München, 2005.
- [29] N. B. Colthup, L. H. Daly, S. E. Wiberley, 'Introduction to Infrared and Raman Spectroscopy', Academic Press, Boston, 1990.
- [30] 'International Tables for X-Ray Crystallography', Vol. C, Kluwer Academic Publisher, Dordrecht, 1992.
- [31] J. Bernstein, R. E. Davis, L. Shimoni, N.-L. Chang, *Angew. Chem., Int. Ed.* **1995**, *34*, 1555.
- [32] RPLUTO, Cambridge Crystallographic Data Centre, Cambridge, UK, 2000, [http://www.ccdc.cam.ac.uk/free\\_services/rpluto/downloads/](http://www.ccdc.cam.ac.uk/free_services/rpluto/downloads/).
- [33] <http://www.bam.de/>.
- [34] T. M. Klapötke, C. M. Rienäcker, *Propellants, Explos., Pyrotech.* **2001**, *26*, 43.
- [35] J. Köhler, R. Meyer, 'Explosivstoffe' 9th edn., Wiley-VCH, Weinheim, Germany, 1998.
- [36] M. S. Westwell, M. S. Searle, D. J. Wales, D. H. Williams, *J. Am. Chem. Soc.* **1995**, *117*, 5013.

- [37] T. Shimanouchi, 'Tables of Molecular Vibrational Frequencies Consolidated', Vol. 1, National Bureau of Standards, Washington, 1972.
- [38] R. P. Singh, R. D. Verma, D. T. Meshri, J. M. Shreeve, *Angew. Chem., Int. Ed.* **2006**, *45*, 3584, and ref cit. therein.
- [39] M. Sućeska, *Propellants, Explos., Pyrotech.* **1991**, *16*, 197.
- [40] L. E. Fried, K. R. Glaesemann, W. M. Howard, P. C. Souers, 'CHEETAH 4.0 User's Manual', Lawrence Livermore National Laboratory, 2004.
- [41] G. I. Koldobskii, D. S. Soldatenko, E. S. Gerasimova, N. R. Khokhryakova, M. B. Shcherbinin, V. P. Lebedev, V. A. Obstrovskii, *Russ. J. Org. Chem.* **1997**, *33*, 1771.
- [42] T. M. Klapötke, C. Miró Sabaté, M. Rasp, *Dalton Trans.* **2009**, 1825; T. M. Klapötke, C. Miró Sabaté, M. Rasp, *J. Mater. Chem.* **2009**, *19*, 2240.
- [43] 'NIST Chemistry WebBook', 2003. Release www version: <http://webbook.nist.gov/chemistry>.
- [44] ICT-Thermodynamic Code, Version 1.0, Fraunhofer-Institut für Chemische Technologie (ICT), Pfintzthal, Germany, 1988–2000; R. Webb, M. van Rooijen, *Proceed. 29th Int. Pyrotech. Sem.*, Westminster, 2002, p. 823; H. Bathelt, F. Volk, *27th Int. Ann. Conf. ICT*, 1996, p. 1.
- [45] C. Darwich, T. M. Klapötke, C. Miró Sabaté, *Chem. – Eur. J.* **2008**, *14*, 5756.
- [46] [http://www.linseis.net/html\\_en/thermal/dsc/dsc\\_pt10.php](http://www.linseis.net/html_en/thermal/dsc/dsc_pt10.php).
- [47] <http://www.perkinelmer.com>.
- [48] CrysAlis CCD, Version 1.171.27p5 beta, Oxford Diffraction Ltd.
- [49] CrysAlis RED, Version 1.171.27p5 beta, Oxford Diffraction Ltd.
- [50] A. Altomare, G. Casciaro, C. Giacovazzo, A. Guagliardi, *J. Appl. Crystallogr.* **1993**, *26*, 343.
- [51] G. M. Sheldrick, SHELXS-97, Program for Crystal Structure Solution, University of Göttingen, Germany, 1994.
- [52] G. M. Sheldrick, SHELXL97, Program for the Refinement of Crystal Structures, University of Göttingen, Germany, 1997.
- [53] L. J. Farrugia, *J. Appl. Crystallogr.* **1999**, *32*, 837.
- [54] A. L. Spek, PLATON, A Multipurpose Crystallographic Tool, Utrecht, The Netherlands, 1999.
- [55] SCALE3 ABSPACK, An Oxford Diffraction Program, Oxford Diffraction Ltd., 2005.
- [56] <http://www.parrinst.com>.
- [57] M. J. Frisch, G. W. Trucks, H. B. Schlegel, G. E. Scuseria, M. A. Robb, J. R. Cheeseman, J. A. Montgomery Jr., T. Vreven, K. N. Kudin, J. C. Burant, J. M. Millam, S. S. Iyengar, J. Tomasi, V. Barone, B. Mennucci, M. Cossi, G. Scalmani, N. Rega, G. A. Petersson, H. Nakatsuji, M. Hada, M. Ehara, K. Toyota, R. Fukuda, J. Hasegawa, M. Ishida, T. Nakajima, Y. Honda, O. Kitao, H. Nakai, M. Klene, X. Li, J. E. Knox, H. P. Hratchian, J. B. Cross, C. Adamo, J. Jaramillo, R. Gomperts, R. E. Stratmann, O. Yazyev, A. J. Austin, R. Cammi, C. Pomelli, J. W. Ochterski, P. Y. Ayala, K. Morokuma, G. A. Voth, P. Salvador, J. J. Dannenberg, V. G. Zakrzewski, S. Dapprich, A. D. Daniels, M. C. Strain, O. Farkas, D. K. Malick, A. D. Rabuck, K. Raghavachari, J. B. Foresman, J. V. Ortiz, Q. Cui, A. G. Baboul, S. Clifford, J. Cioslowski, B. B. Stefanov, G. Liu, A. Liashenko, P. Piskorz, I. Komaromi, R. L. Martin, D. J. Fox, T. Keith, M. A. Al-Laham, C. Y. Peng, A. Nanayakkara, M. Challacombe, P. M. W. Gill, B. Johnson, W. Chen, M. W. Wong, C. González, J. A. Pople, Gaussian 03, Revision A.1, Gaussian, Inc., Pittsburgh, 2003.
- [58] J. A. Pople, R. Seeger, R. Krishnan, *Int. J. Quantum Chem.* **1977**, *S11*, 149.
- [59] R. A. Kendall, T. H. Dunning Jr., R. J. Harrison, *J. Chem. Phys.* **1992**, *96*, 6796.
- [60] K. A. Peterson, D. E. Woon, T. H. Dunning Jr., *J. Chem. Phys.* **1994**, *100*, 7410.

Received October 22, 2008